Article

Cell Metabolism

A Liver-Bone Endocrine Relay by IGFBP1 Promotes Osteoclastogenesis and Mediates FGF21-Induced Bone Resorption

Graphical Abstract

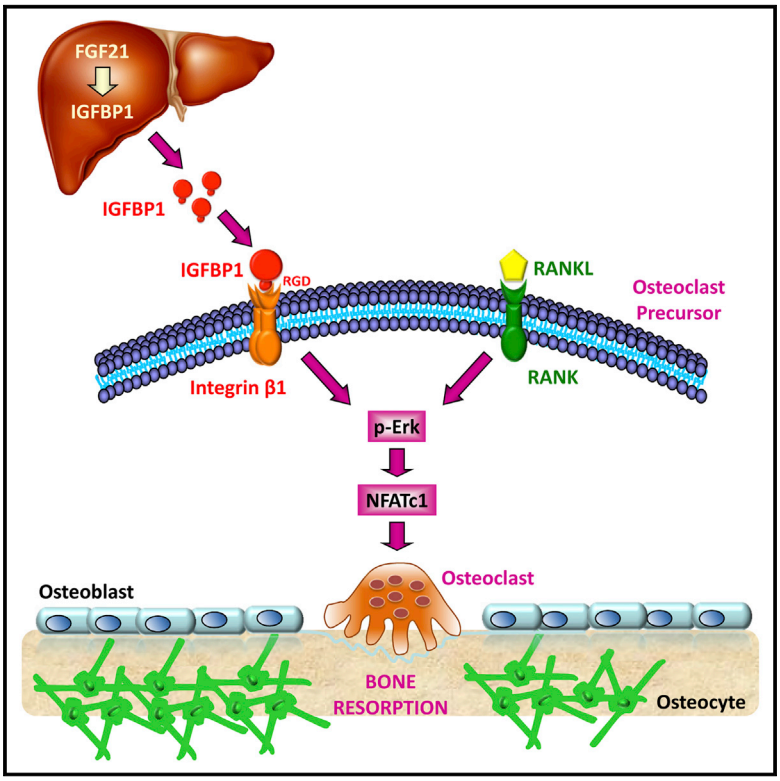

Authors

Xunde Wang, Wei Wei, Jing Y. Krzeszinski, Yubao Wang, Yihong Wan

Correspondence

yihong.wan@utsouthwestern.edu

In Brief

Wang et al. uncover IGFBP1 as a liver hormone that activates Integrin β1 receptor to stimulate osteoclast differentiation and bone degradation in response to metabolic cues such as FGF21. IGFBP1 blockade is a potential strategy to prevent FGF21-induced bone loss while retaining its metabolic benefits.

Highlights

- IGFBP1 is an FGF21-induced pro-osteoclastogenic liver hormone
- IGFBP1 functions through Integrin β1 receptor in the osteoclast lineage
- IGFBP1 potentiates RANKL signaling and NFATc1 activation
- IGFBP1 blockade abolishes FGF21-induced bone resorption but not insulin sensitization

Wang et al., 2015, Cell Metabolism *22*, 811–824
November 3, 2015 ©2015 Elsevier Inc.
http://dx.doi.org/10.1016/j.cmet.2015.09.010

CellPress

A Liver-Bone Endocrine Relay by IGFBP1 Promotes Osteoclastogenesis and Mediates FGF21-Induced Bone Resorption

Xunde Wang,[1,2] Wei Wei,[1,2] Jing Y. Krzeszinski,[1] Yubao Wang,[1] and Yihong Wan[1,*]
[1]Department of Pharmacology, University of Texas Southwestern Medical Center, Dallas, TX 75390, USA
[2]Co-first author
*Correspondence: yihong.wan@utsouthwestern.edu
http://dx.doi.org/10.1016/j.cmet.2015.09.010

SUMMARY

Fibroblast growth factor 21 (FGF21) promotes insulin sensitivity but causes bone loss. It elevates bone resorption by an undefined non-osteoclast-autonomous mechanism. We have detected a pro-osteoclastogenic activity in the hepatic secretome that is increased by FGF21 and largely attributed to insulin-like growth factor binding protein 1 (IGFBP1). Ex vivo osteoclast differentiation and in vivo bone resorption are both enhanced by recombinant IGFBP1 but suppressed by an IGFBP1-blocking antibody. Anti-IGFBP1 treatment attenuates ovariectomy-induced osteoporosis and abolishes FGF21-induced bone loss while maintaining its insulin-sensitizing metabolic benefit. Mechanistically, IGFBP1 functions via its RGD domain to bind to its receptor integrin β1 on osteoclast precursors, thereby potentiating RANKL-stimulated Erk-phosphorylation and NFATc1 activation. Consequently, osteoclastic integrin β1 deletion confers resistance to the resorption-enhancing effects of both IGFBP1 and FGF21. Therefore, the hepatokine IGFBP1 is a critical liver-bone hormonal relay that promotes osteoclastogenesis and bone resorption as well as an essential mediator of FGF21-induced bone loss.

INTRODUCTION

Osteoclasts, the professional bone resorbing cells, are essential for bone turnover and skeletal regeneration (Novack and Teitelbaum, 2008). However, excessive osteoclast activity can lead to diseases such as osteoporosis, arthritis, and cancer bone metastasis (Novack and Teitelbaum, 2008). Osteoclastogenesis is the differentiation of osteoclasts from hematopoietic progenitors in response to receptor activator of nuclear factor kappa-B ligand (RANKL), which can be regulated by endocrine hormones and metabolic signals. It can also be stimulated by pharmacological agents such as rosiglitazone, a widely used drug for diabetes (Wan et al., 2007). New knowledge of how osteoclastogenesis and bone resorption are regulated will provide key insights into disease pathology as well as better treatment.

FGF21 is a powerful regulator of glucose and lipid metabolism, thus a potential new drug for obesity and diabetes that is currently in clinical trials (Cantó and Auwerx, 2012; Potthoff et al., 2012). We have recently identified FGF21 as a physiologically and pharmacologically significant negative regulator of bone mass (Wei et al., 2012), suggesting that skeletal fragility may be an undesirable consequence of chronic FGF21 administration. Thus, the identification of the cellular and molecular mechanisms for how FGF21 controls bone homeostasis will both enhance our fundamental understanding of skeletal physiology and illuminate potential strategies to separate its metabolic benefits from its detrimental bone loss side effects.

FGF21 induces bone loss by simultaneously decreasing bone formation and increasing bone resorption (Wei et al., 2012). However, the mechanism for how FGF21 enhances bone resorption was unclear. Our previous findings show that FGF21 does not directly regulate osteoclast differentiation from hematopoietic progenitors (Wei et al., 2012), indicating that FGF21 acts on other tissues and cell types to indirectly promote osteoclastogenesis and bone resorption. Here we have identified IGFBP1 as an endocrine hormone from the liver that directly promotes RANKL-mediated osteoclastogenesis via its receptor integrin β1, as well as an essential mediator of FGF21-induced bone resorption and bone loss.

RESULTS

IGFBP1 Is an FGF21-Induced Pro-Osteoclastogenic Hepatokine

Because FGF21 is highly expressed in the liver, we hypothesize that it may induce the secretion of endocrine factor(s) from the liver that can directly enhance osteoclastogenesis. To test this hypothesis, we collected an liver-cell-derived conditioned medium (LCM) from wild-type (WT) or FGF21-Tg mice and determined their effects on RANKL-mediated and rosiglitazone-stimulated osteoclast differentiation from WT bone marrow cells. Compared with mock treatment, osteoclast differentiation was significantly augmented by LCM from WT mice and further enhanced by LCM from FGF21-Tg mice, quantified by the expression of osteoclast markers such as tartrate-resistant acid phosphatase (TRAP) (Figure 1A). These results indicate that WT liver secrets pro-osteoclastogenic factor(s) in response to physiological levels of FGF21, which is enhanced by pharmacological FGF21 overexpression.

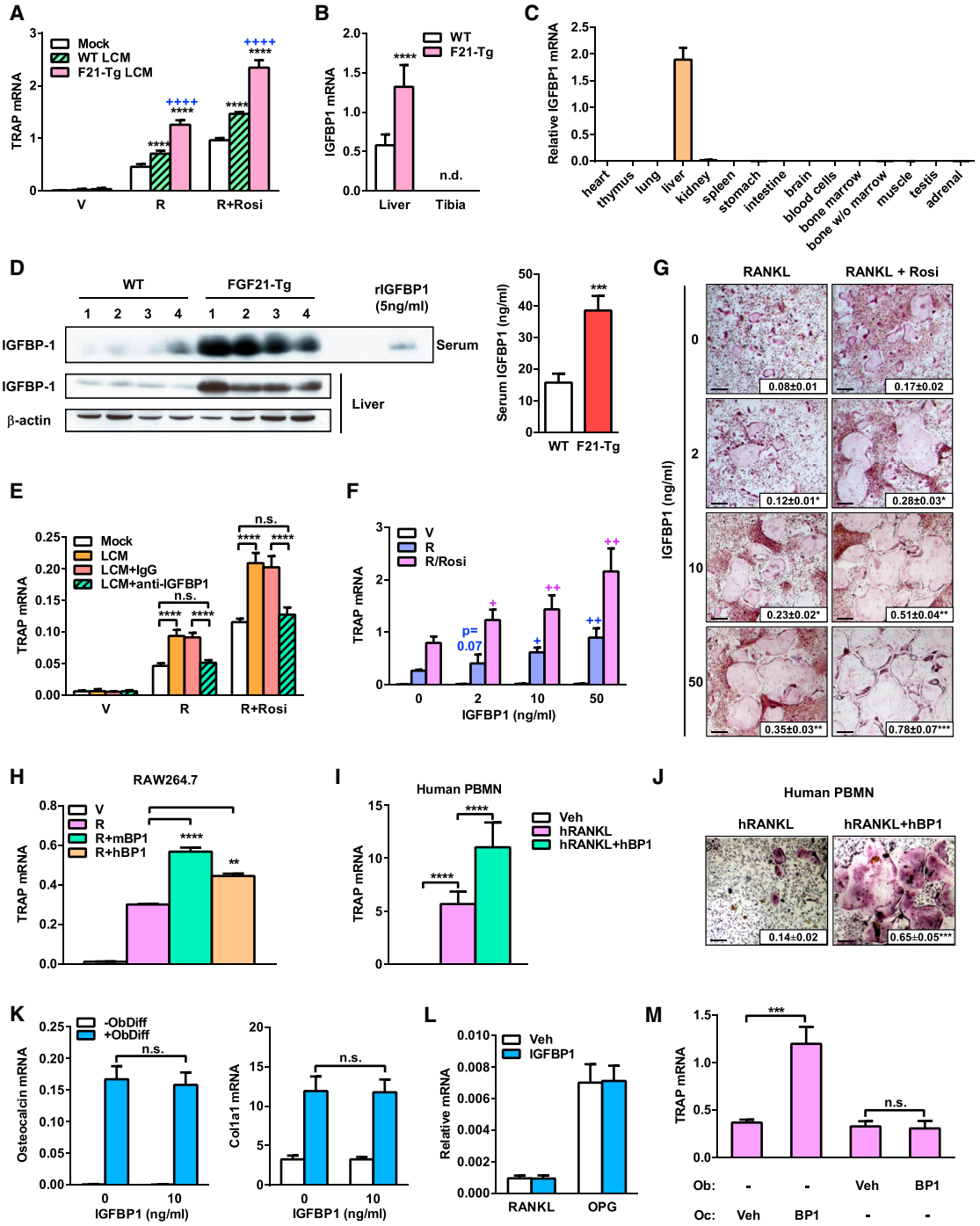

Figure 1. IGFBP1 Is an FGF21-Induced Pro-Osteoclastogenic Hepatokine

(A) Effects of LCM from WT or FGF21-Tg mice (2-month-old, male, n = 4) on osteoclast differentiation from WT bone marrow cells, quantified by the mRNA of a representative osteoclast marker TRAP (n = 4); * compares LCM treatment with mock controls; + compares LCM from FGF21-Tg mice with LCM from WT control mice. V, vehicle; R, RANKL; Rosi, rosiglitazone.

(B) IGFBP1 mRNA levels in the liver and tibia (bone + marrow) from WT and FGF21-Tg mice (n = 3); n.d., not detected.

(C) IGFBP1 mRNA levels in various tissues (n = 3).

(D) (Left) Western blot of IGFBP1 protein in the serum (top) and liver (bottom) of WT and FGF21-Tg mice (2-month-old, male, n = 4). Equal volume (20 μl) of each sample and rIGFBP1 was loaded; the concentration of rIGFBP1 used (5 ng/ml) is shown. (Right) ELISA of serum IGFBP1 levels in WT and FGF21-Tg mice (2-month-old, male, n = 6).

(E) The pro-osteoclastogenic activity of WT LCM was abolished by an IGFBP1-blocking antibody (anti-IGFBP1, 100 ng/ml) (n = 3). IgG served as a negative control.

(legend continued on next page)

To identify this pro-osteoclastogenic hepatokine, we searched for liver-specific secreted factors that are upregulated by FGF21. Because IGFBP1 is an FGF21-inducible liver-specific factor (Inagaki et al., 2008), and osteoclast differentiation can be enhanced by the predominantly osteoblast-residing IGFBP2 (DeMambro et al., 2012), we postulate that IGFBP1 may be the pro-osteoclastogenic hepatokine in the LCM that is responsible for FGF21-induced bone resorption. We found that IGFBP1 mRNA was high and FGF21 inducible in the liver but absent in the bone (Figure 1B). Liver IGFBP1 mRNA was lower in FGF21-KO mice (Figure S1A), suggesting that FGF21 induction of IGFBP1 is physiologically relevant. IGFBP1 mRNA was the highest in the liver compared to other tissues by >100-fold (Figure 1C), supporting its role as a hepatokine. Moreover, IGFBP1 protein levels in both liver and serum were increased in FGF21-Tg mice compared to WT controls (Figure 1D). These results show that FGF21 induces IGFBP1 expression and secretion from the liver.

To investigate whether IGFBP1 is required for the pro-osteoclastogenic activity in WT LCM, we tested whether the activity can be eliminated by an IGFBP1-blocking antibody. Compared to an IgG control, anti-IGFBP1 abolished the osteoclast-enhancing effects of WT LCM (Figure 1E). Western blot confirmed that anti-IGFBP1 did not cross-react with IGFBP2 (Figure S1B). These results indicate that IGFBP1 is the major pro-osteoclastogenic factor in the liver secretome.

To determine if IGFBP1 is sufficient to stimulate RANKL-mediated osteoclastogenesis in the absence of other factors in the liver secretome, we next treated WT osteoclast differentiation cultures with recombinant IGFBP1. When bone marrow osteoclast differentiation was induced with 100 ng/ml RANKL, IGFBP1 significantly stimulated osteoclast differentiation at 2 ng/ml, and the effects were enhanced in a dose-dependent manner, shown by the increased TRAP expression (Figure 1F), number and size of mature osteoclasts, as well as resorptive activity (Figure 1G). A titration of anti-IGFBP1 antibody showed that the pro-osteoclastogenic effects by 2 ng/ml IGFBP1 could be completely blocked by 4 ng/ml of anti-IGFBP1 (Figure S1C). Moreover, RANKL-induced osteoclast differentiation from the RAW264.7 mouse macrophage cell line was also enhanced by both mouse and human IGFBP1 (Figure 1H).

To determine whether IGFBP1 also regulates osteoclast differentiation in human cells, we treated human peripheral blood mononuclear (PBMN) precursors with human RANKL, in the presence of human IGFBP1 or vehicle control. Osteoclast differentiation from human PBMN was also augmented by hIGFBP1, shown by the higher TRAP expression (Figure 1I), as well as the increased number, size, and activity of mature osteoclasts (Figure 1J).

In contrast, IGFBP1 affected neither bone marrow osteoblast differentiation (Figure 1K) nor RANKL/OPG expression in osteoblasts (Figure 1L). When osteoblast-derived conditioned medium was applied to osteoclast cultures, osteoclastogenesis was enhanced only when IGFBP1 was added to osteoclasts but not osteoblasts, further indicating that IGFBP1 acts directly on osteoclasts rather than indirectly through osteoblasts (Figure 1M). Collectively, these findings indicate that IGFBP1 is a pro-osteoclastogenic hepatokine that is induced by FGF21 and functions as an endocrine hormone upon the skeleton.

Bone Resorption Is Enhanced by rIGFBP1 but Blocked by Anti-IGFBP1 Antibody

We next investigated whether IGFBP1 gain- or loss-of-function regulates bone resorption in vivo. For gain-of-function, we administered recombinant IGFBP1 into WT mice with a daily immunoprecipitation (IP) injection at 0.015 mg/kg/day for 14 days. For loss of function, we administered an IGFBP1 blocking antibody into WT mice with a daily IP injection at 0.03 mg/kg/day for 14 days. ELISA analysis of a bone resorption marker C-terminal telopeptide fragments of the type I collagen (CTX-1) revealed that bone resorption was increased by 110% by rIGFBP1 and decreased by 42% by anti-IGFBP1 compared with control (Figure 2A). Consistent with our ex vivo observation that IGFBP1 does not affect osteoblast differentiation (Figure 1L), the bone formation marker N-terminal propeptide of type I procollagen (P1NP) was unaltered by either rIGFBP1 or anti-IGFBP1

(F and G) Recombinant mouse IGFBP1 enhanced the RANKL-mediated and rosiglitazone-stimulated osteoclast differentiation from WT bone marrow cells in a dose-dependent manner.

(F) Quantification of TRAP mRNA (n = 3); $^{+}$ compares IGFBP1 treatment with no IGFBP1 controls.

(G) Representative images of TRAP-stained differentiation cultures showing that IGFBP1 increased the number and size of mature osteoclasts at day 4 after RANKL treatment. Mature osteoclasts were identified as multinucleated (>3 nuclei) TRAP^{+} (purple) cells. Scale bar, 25 μm. Inset shows the quantification of resorptive activity by calcium release from bone into medium (mM) (n = 8); * compares with no IGFBP1 control.

(H) Osteoclast differentiation from RAW264.7 mouse macrophage cell line was induced by RANKL and further enhanced by mouse and human IGFBP1, quantified by TRAP mRNA (n = 3). R, RANKL; BP1, IGFBP1.

(I and J) Osteoclast differentiation from human PBMN cells was induced by human RANKL and further enhanced by human IGFBP1.

(I) Quantification of TRAP mRNA (n = 3).

(J) Representative images of TRAP-stained differentiation cultures. Scale bar, 25 μm. Inset shows resorptive activity by calcium release from bone into medium (mM) (n = 8); * compares IGFBP1 with vehicle control.

(K–M) IGFBP1 does not affect osteoblast differentiation or RANKL/OPG expression.

(K and L) Bone marrow osteoblast differentiation cultures were treated with 0 or 10 ng/ml of IGFBP1.

(K) Osteoblast differentiation was unaltered, quantified by the mRNA of osteoblast markers osteocalcin and Col1a1 (n = 3). ObDiff, osteoblast differentiation cocktail.

(L) RANKL and OPG expression in osteoblasts were unaltered by IGFBP1 (n = 3).

(M) Bone marrow osteoblast differentiation cultures were treated with 50 ng/ml IGFBP1 or vehicle control (Veh) for 18 days; on the last day, the cells were cultures in fresh medium without IGFBP1 for 16 hr, and osteoblast conditioned medium was collected and added to osteoclast differentiation cultures together with 50 ng/ml IGFBP1 or Veh control, in the presence of 20 ng/ml RANKL. Osteoclast differentiation was quantified as TRAP expression (n = 3).

Statistical analyses were performed with Student's t test and are shown as mean ± SD. *$p < 0.05$; **$p < 0.01$; ***$p < 0.005$; ****$p < 0.001$; n.s., non-significant ($p > 0.05$). See also Figure S1.

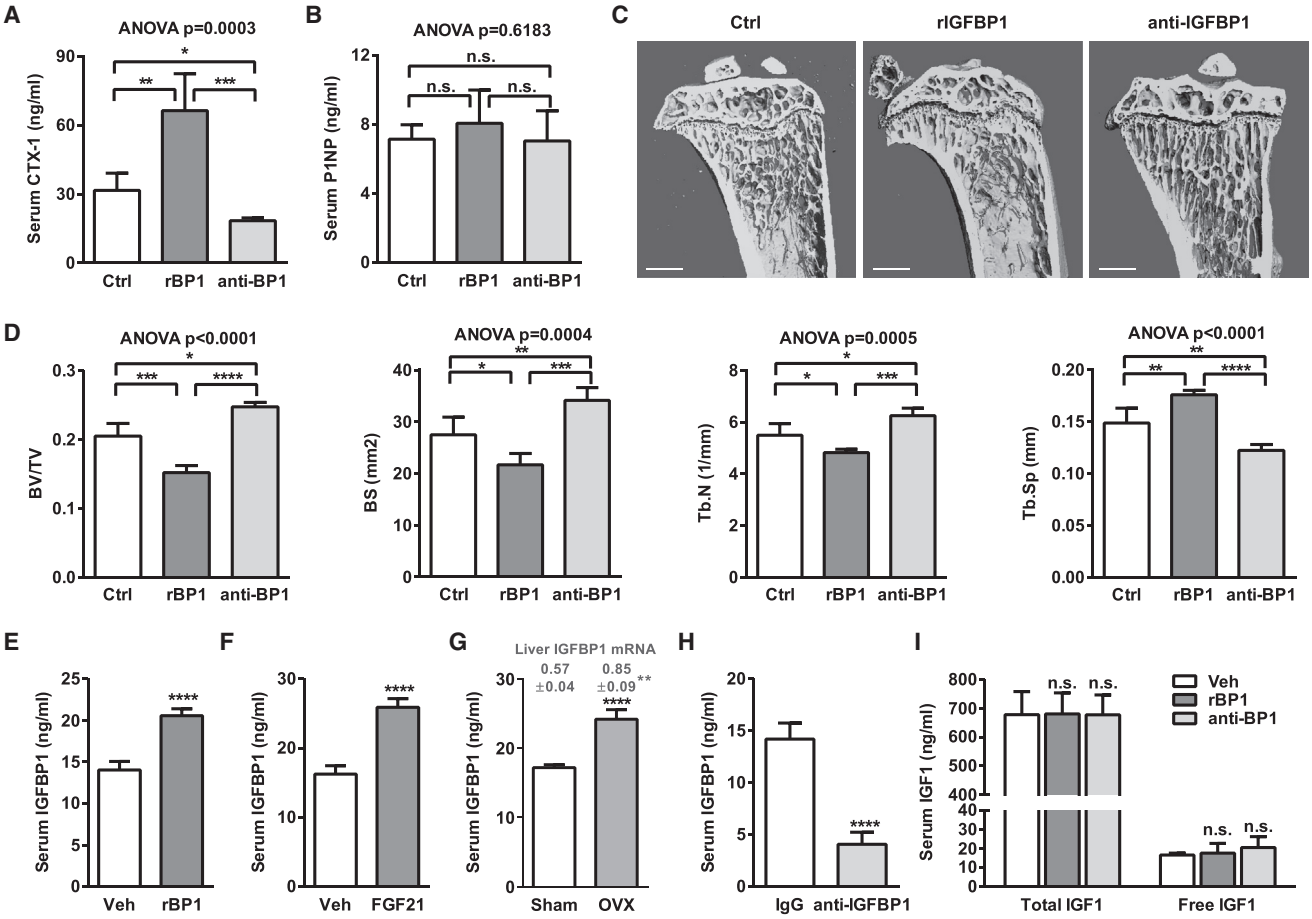

Figure 2. IGFBP1 Enhances Bone Resorption In Vivo

(A–D) Effects of rIGFBP1 and anti-IGFBP1 treatment on bone. WT C57BL6 mice (10-week-old, male, n = 6) were treated with IGFBP1 (0.015 mg/kg/day), anti-IGFBP1 antibody (0.03 mg/kg/day), or control by daily IP injection for 14 days. PBS and IgG controls showed similar results, and representative data for PBS control are shown.

(A) Serum CTX-1 bone resorption marker.

(B) Serum P1NP bone formation marker.

(C) Representative μCT images of the entire proximal tibiae (scale bar, 1 mm).

(D) Quantification of trabecular bone volume and architecture. BV/TV, bone volume/tissue volume ratio; BS, bone surface; Tb.N, trabecular number; Tb.Sp, trabecular separation.

(E–H) ELISA analyses of serum IGFBP1 levels.

(E) WT C57BL6 mice (10-week-old, male, n = 6) were treated with PBS vehicle control (Veh) or IGFBP1 (0.015 mg/kg/day) for 14 days.

(F) WT C57BL6 mice (3-month-old, male, n = 6) were fed with HFD for 5 weeks and treated with vehicle or FGF21 (1 mg/kg/day) for the last 14 days.

(G) WT C57BL6 mice (4-month-old, female, n = 6) were OVX or sham-operated, and serum was collected 5 weeks later. Liver IGFBP1 mRNA level was also higher in OVX mice compared with sham controls (shown on top). IGFBP1 mRNA in other tissues such as kidney, heart, bone, bone marrow, spleen, thymus, lung, stomach, intestine, brain, and muscle were below 0.005 and not significantly different between OVX and sham.

(H) Serum IGFBP1 was reduced by anti-IGFBP1 treatment. WT C57BL6 mice (10-week-old, male, n = 6) were treated with IgG control or anti-IGFBP1 (0.03 mg/kg/day) for 14 days. Antibody-bound IGFBP1 in the serum was removed by protein A/G plus agarose, and then unbound IGFBP1 was quantified.

(I) Serum levels of total IGF1 and free IGF1 were unaffected by rIGFBP1 or anti-IGFBP1 treatment, quantified by ELISA. WT C57BL6 mice (10-week-old, male, n = 6) were treated with rIGFBP1 (0.015 mg/kg/day), anti-IGFBP1 (0.03 mg/kg/day), or vehicle control for 14 days.

Statistical analyses were performed with ANOVA followed by the post hoc Tukey pairwise comparisons ([A]–[D]) or Student's t test ([E]–[I]); error bars indicate SD. *$p < 0.05$; **$p < 0.01$; ***$p < 0.005$; ****$p < 0.001$; n.s., non-significant ($p > 0.05$). See also Figure S2.

treatment (Figure 2B). Histomorphometry showed that osteoclast numbers and surface, as well as eroded surface, were increased by rIGFBP1 and decreased by anti-IGFBP1 (Figure S2A), whereas osteoblast numbers and surface, as well as bone formation rate and mineral apposition rate, were unaltered (Figures S2B and S2C). Consequently, micro-computed tomography (μCT) analysis of the proximal tibiae revealed that IGFBP1 treatment caused a significant bone loss; in contrast, anti-IGFBP1 treatment protected bone leading to a significantly higher bone mass (Figures 2C, 2D, and S2D).

Two weeks of rIGFBP1 treatment elevated serum IGFBP1 by 47% (Figure 2E), which was similar to the IGFBP1 induction by 2 weeks of FGF21 treatment (59%) (Figure 2F). Interestingly, we found that ovariectomy (OVX)—a widely used model for

postmenopausal osteoporosis—also elevated serum IGFBP1 levels in female mice to a similar degree by 41% compared with sham controls (Figure 2G). This stemmed from a 49% increase in hepatic IGFBP1 expression (Figure 2G, top) as IGFBP1 expression in other tissues were >100-fold lower and unaffected by OVX. This is consistent with human studies showing elevated plasma IGFBP1 levels in osteoporotic patients (Jehle et al., 2003; Salminen et al., 2008). Conversely, 2 weeks of anti-IGFBP1 treatment reduced serum IGFBP1 by 71% (Figure 2H).

Importantly, serum levels of free and total IGF1 were unaltered by rIGFBP1 or anti-IGFBP1 treatment at the dose applied (Figure 2I), consistent with the result that bone formation was unchanged. This observation is in line with the fact that IGFBP3 is the most abundant circulating IGFBP that accounts for 80%–90% of all IGF binding (Key et al., 2010; Stolzenberg-Solomon et al., 2004), and IGFBP1 only plays a minor role in IGF1 sequestration. Moreover, the anti-IGFBP1 antibody exhibits <1% cross-reactivity with other IGFBPs such as IGFBP-2, IGFBP-3, IGFBP-5, IGFBP-6, and IGFBP-7 (R&D Systems; Figure S1B). Therefore, our pharmacological approaches to acutely increase or decrease IGFBP1 levels during adulthood at a physiologically relevant dose presents a unique window of opportunity to examine the intrinsic function of IGFBP1 in vivo that is independent of IGF1, revealing it as a potent resorption-enhancing liver hormone.

IGFBP1 Blockade Abolishes OVX-Induced Bone Resorption

To further explore the therapeutic potential of IGFBP1 blockade, we examined whether anti-IGFBP1 treatment can attenuate the elevated bone resorption during postmenopausal osteoporosis in a mouse disease model. To simulate the estrogen loss in postmenopausal women, we performed OVX in female WT mice. Three days after OVX or sham surgery, we injected anti-IGFBP1 or an IgG-negative control at 0.03 mg/kg and three times per week for 5 weeks. Uterine weight was reduced by ~80% in all OVX mice compared to sham controls, indicating effective estrogen depletion (Figure 3A). Serum CTX-1 was increased by 55% in OVX mice treated with IgG control compared to sham control mice treated with IgG (Figure 3B). In contrast, the OVX-induced bone resorption was abolished by anti-IGFBP1 treatment, which instead led to a 28% reduction in CTX-1 compared to sham controls treated with IgG (Figure 3B). Although bone formation was unaffected by anti-IGFBP1 treatment (Figure 3C), OVX-induced bone loss was significantly rescued (Figure 3D). Body weight in OVX mice was unaffected by anti-IGFBP1 treatment (not shown). These results reveal an additional mechanism for OVX-induced bone resorption: estrogen loss exerts not only a direct effect of enhancing osteoclast survival (Krum, 2011; Nakamura et al., 2007) but also an indirect effect of increasing osteoclast differentiation via elevating circulating IGFBP1 levels, suggesting that IGFBP1 blockade may be a potential treatment for osteoporosis.

IGFBP1 Blockade Abolishes FGF21-Induced Bone Resorption

We also tested if anti-IGFBP1 could ameliorate the bone resorption induced by FGF21. Under chow-diet feeding, anti-IGFBP1 (0.03 mg/kg/day for 14 days) effectively reduced serum CTX-1 in FGF21-Tg mice to a similar level as in WT controls (Figure 3E), without affecting serum P1NP (Figure 3F), leading to a significant rescue of the FGF21-induced bone loss (Figure 3G). Histomorphometry showed that this anti-IGFBP1 treatment abolished the increased osteoclast surface and number in FGF21-Tg mice (Figure S3A) without significantly affecting osteoblast surface/number, bone formation rate, or mineral apposition rate (Figures S3B and S3C). Similarly, under high-fat diet (HFD) feeding, anti-IGFBP1 also prevented FGF21 induction of CTX-1 (Figure 3H), without affecting FGF21 reduction of P1NP (Figure 3I), leading to the attenuation of FGF21-induced bone loss (Figure 3J). Importantly, insulin tolerance test (ITT) showed that the improved insulin sensitivity in FGF21-Tg mice was intact following anti-IGFBP1 treatment (Figure 3K). This indicates that IGFBP1 blockade may represent an exciting strategy to prevent the bone loss side effects while retaining the metabolic benefits of FGF21.

IGFBP1 Potentiates RANKL-Stimulated Erk Phosphorylation and NFATc1 Activation

We next investigated the molecular mechanisms for how IGFBP1 enhances osteoclastogenesis. Our bone marrow osteoclast differentiation scheme allowed us to specifically dissect the effects of IGFBP1 on precursor proliferation during the first 3 days of MCSF treatment (d1–3), and osteoclast differentiation during the latter 3 days of RANKL + MCSF treatment (d4–6) (Figure 4A). When IGFBP1 treatment was limited to d4–6 only, osteoclast differentiation was enhanced to a similar extent as when IGFBP1 treatment was throughout the entire 6 days (d1–6) (Figures 4B and S1D). In contrast, osteoclast differentiation was unaffected when IGFBP1 treatment was limited to d1–3 (Figures 4B and S1D). Consistent with these observations, MTT assay showed that IGFBP1 did not alter cell proliferation on either d3 or d6 (Figure 4C). These results indicate that IGFBP1 promotes osteoclastogenesis by enhancing RANKL-mediated differentiation without affecting MCSF-mediated precursor proliferation.

We next examined how IGFBP1 potentiates RANKL signaling. We found that IGFBP1 enhanced both basal and RANKL-induced Erk phosphorylation in osteoclast differentiation cultures (Figures 4D and 4E). In contrast, IGFBP1 did not affect basal or RANKL-stimulated c-Jun phosphorylation, Akt phosphorylation, or IκBα degradation (Figure 4F). To identify which RANKL downstream transcription factor(s) is regulated by IGFBP1 signaling, we transfected RAW267.4 cells with a luciferase reporter driven by the response elements for NFATc1, AP-1, or NF-κB. As expected, RANKL treatment activated these endogenous transcription factors, leading to the induction of their corresponding luciferase reporter (Figure 4G). IGFBP1 co-treatment selectively potentiated the RANKL-induction of NFATc1 reporter, but not AP-1 or NFκB reporters (Figure 4G). In line with the published reports that Erk activation promotes NFATc1 signaling and osteoclast differentiation (Choi et al., 2014; Kim et al., 2007), our results showed that IGFBP1 enhancement of NFATc1 and osteoclastogenesis was abolished by an Erk inhibitor (Figure 4H). Consistently, IGFBP1 also increased NFATc1 expression in osteoclast differentiation cultures (Figure 4I). These results indicate that IGFBP1 promotes RANKL-mediated osteoclastogenesis by enhancing Erk phosphorylation and NFATc1 activation.

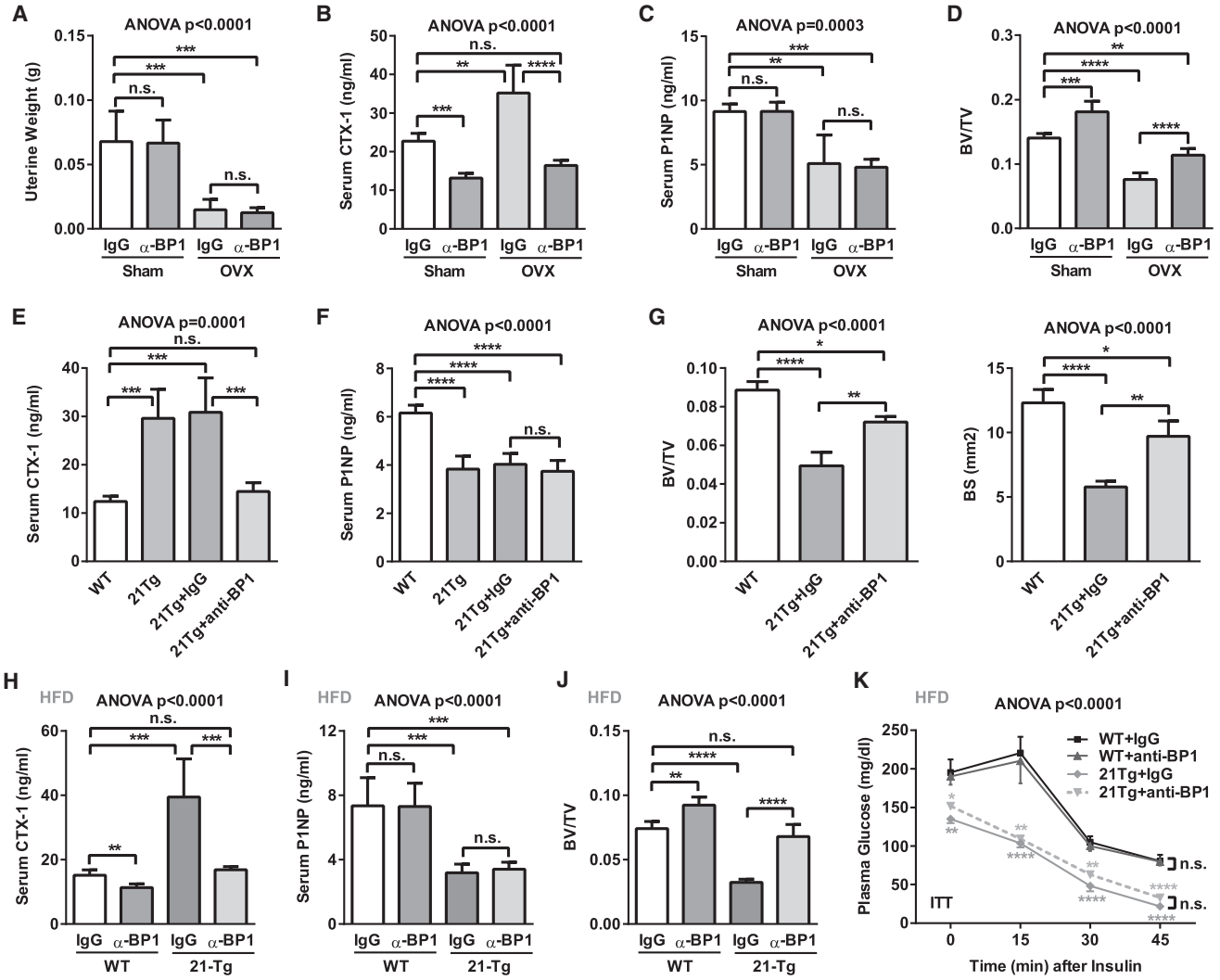

Figure 3. IGFBP1 Blockade Abolishes OVX- and FGF21-Induced Bone Resorption

(A–D) Anti-IGFBP1 treatment attenuates OVX-induced bone resorption and bone loss. WT C57BL6 mice (18-week-old, female, n = 6) were OVX or sham-operated. Three days after surgery, they were treated with anti-IGFBP1 (anti-BP1) or IgG control at 0.03 mg/kg/day and three times per week for 5 weeks.

(A) Uterine weight.

(B) Serum CTX-1.

(C) Serum P1NP.

(D) BV/TV by μCT.

(E–K) Anti-IGFBP1 treatment attenuates FGF21-induced bone resorption and bone loss.

(E–G) All mice were 7- to 8-month-old females on chow diet (n = 6). FGF21-Tg mice were treated with anti-IGFBP1 (anti-BP1) or IgG control at 0.03 mg/kg/day daily for 14 days and compared with WT mice or untreated FGF21-Tg mice.

(E) Serum CTX-1.

(F) Serum P1NP.

(G) Trabecular BV/TV and BS in proximal tibiae by μCT.

(H–K) All mice were 9- to 10-month-old females that were on HFD for 5 weeks (n = 6). WT or FGF21-Tg mice were treated with anti-IGFBP1 or IgG control at 0.03 mg/kg/day daily for the last 14 days.

(H) Serum CTX-1.

(I) Serum P1NP.

(J) BV/TV.

(K) ITT; * compares with IgG-treated WT mice.

Statistical analyses were performed with ANOVA followed by the post hoc Tukey pairwise comparisons; error bars indicate SD. *$p < 0.05$; **$p < 0.01$; ***$p < 0.005$; ****$p < 0.001$; n.s., non-significant ($p > 0.05$). See also Figure S3.

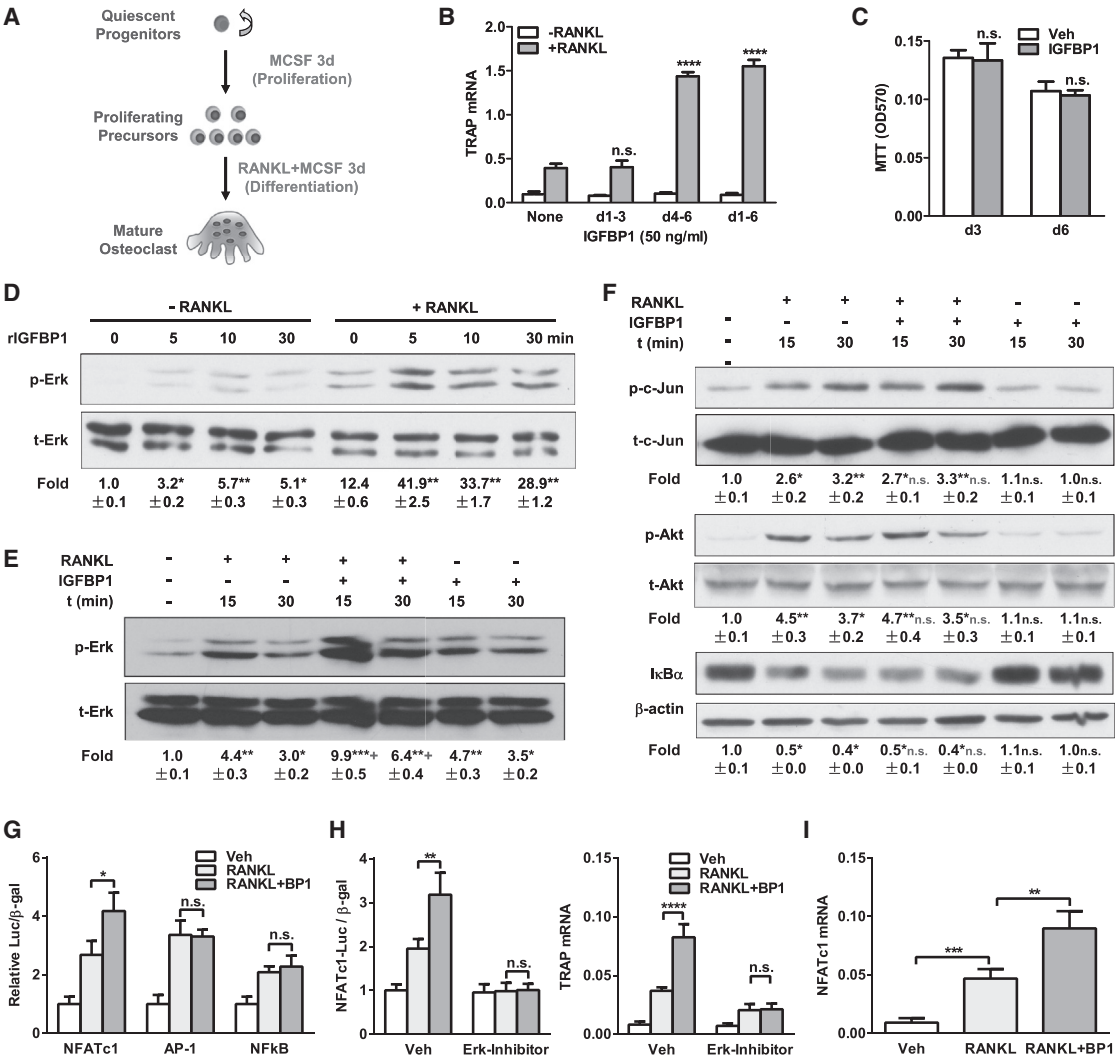

Figure 4. IGFBP1 Potentiates RANKL Signaling by Enhancing Erk-phosphorylation and NFATc1 Activation

(A) A diagram of the time course of the bone marrow osteoclast differentiation assay. d, day.

(B) IGFBP1 functions at the RANKL-induced differentiation stage. IGFBP1 was added to WT osteoclast differentiation cultures on d1–3 only, d4–6 only, or the entire d1–6; differentiation was quantified by TRAP mRNA (n = 3). * and n.s. compare with "no IGFBP1 treatment."

(C) IGFBP1 does not affect cell proliferation in the osteoclast differentiation culture by MTT assays (n = 6).

(D–F) IGFBP1 induces ERK phosphorylation in synergy with RANKL.

(D) WT bone marrow cells were cultured with MCSF for 5 days, with or without RANKL during the last 2 days. The cells were treated with IGFBP1 (50 ng/ml) for the indicated amount of time; the levels of p-ERK and total ERK (t-ERK) were analyzed by western blot. The p-ERK/t-ERK ratio was quantified as fold changes compared to lane 1 (n = 3). * compares with "0 min" time point in each group.

(E and F) WT bone marrow cells were cultured with MCSF for 3 days and then treated with IGFBP1 (50 ng/ml) and/or RANKL (100 ng/ml) for the indicated amount of time.

(E) The p-ERK/t-ERK ratio was quantified as fold changes compared to lane 1 (n = 3).

(F) IGFBP1 does not affect basal or RANKL-induced c-Jun phosphorylation (Ser73), Akt phosphorylation, or IκBα degradation. The p-c-Jun/t-c-Jun ratio, p-Akt/t-Akt ratio, and IκBα/β-actin ratio were quantified as fold changes compared to lane 1 (n = 3). * compares with lane 1; + or n.s. compares with "no IGFBP1" under the same treatment condition.

(G) IGFBP1 specifically enhances RANKL-induced NFATc1 activation. RAW264.7 cells were transfected with NFATc1-Luc, AP1-Luc, or NF-κB-Luc reporter together with a CMV-βgal reporter as internal control for 24 hr and then treated with RANKL (100 ng/ml) and/or IGFBP1 (50 ng/ml) for 24 hr before reporter assays (n = 6).

(H) IGFBP1 enhancement of NFATc1-luc reporter (left) and bone marrow osteoclast differentiation (right) was abolished by Erk inhibitor U0126 (n = 3, 10 μM). Vehicle control (Veh) was PBS+DMSO.

(I) IGFBP1 increased NFATc1 expression in osteoclast differentiation cultures (n = 3).

Statistical analyses were performed with Student's t test and are shown as mean ± SD. *$p < 0.05$; **$p < 0.01$; ***$p < 0.005$; ****$p < 0.001$; n.s., non-significant ($p > 0.05$). See also Figure S1.

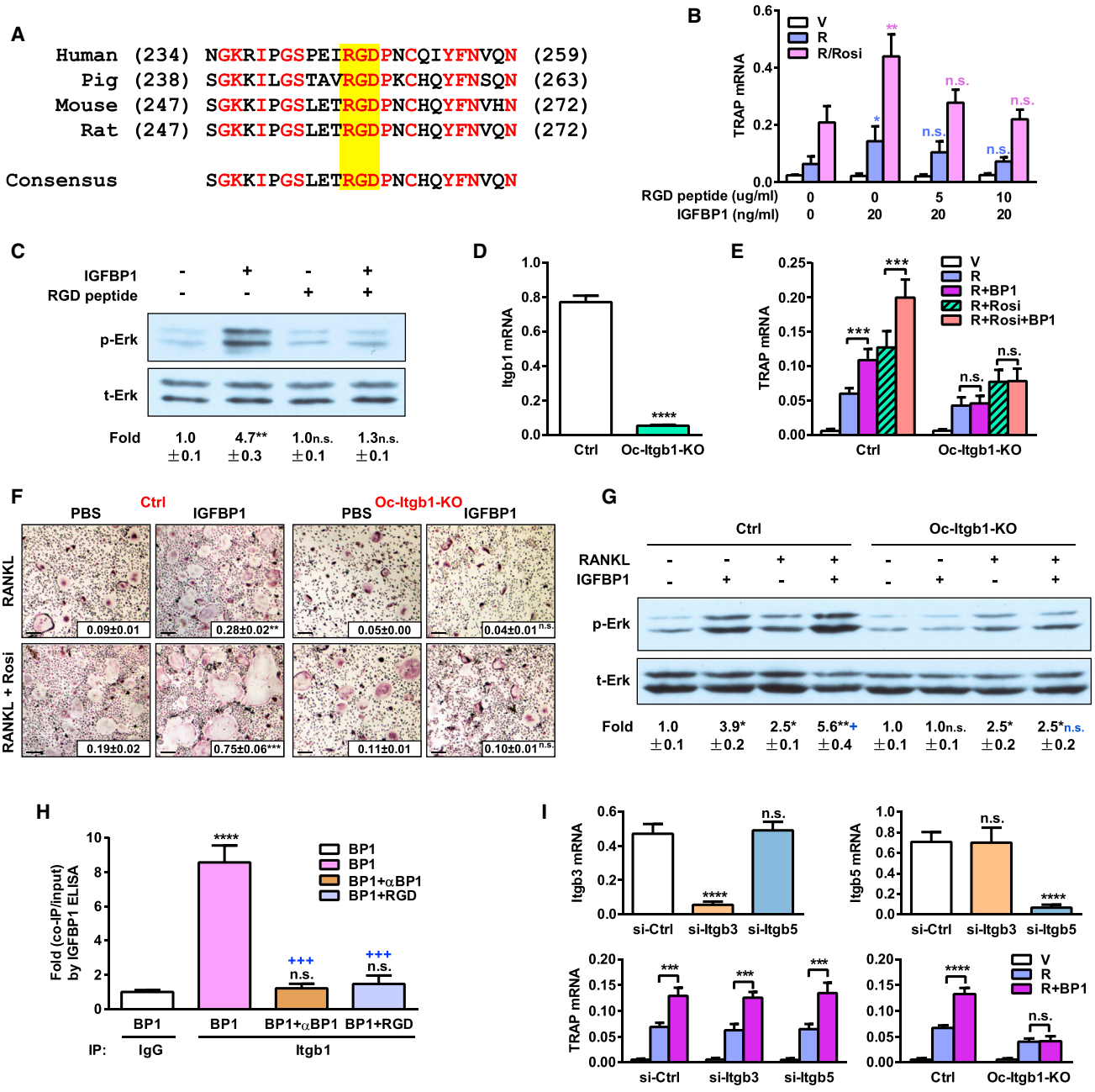

Figure 5. IGFBP1 Functions via Integrin β1 Receptor in Osteoclasts

(A) Amino acid sequence alignment of the C-termini of IGFBP1 from human, pig, mouse, and rat. The conserved amino acids are highlighted in red; the RGD motifs are highlighted in yellow.

(B) An RGD-containing peptide dose-dependently abolished the pro-osteoclastogenic activity of IGFBP1, quantified by TRAP mRNA (n = 3). * and n.s. compare with "no IGFBP1 treatment" (the group on the most left side) under the same RANKL (R) or Rosi treatment condition.

(C) IGFBP1-induced ERK phosphorylation was abolished by RGD-containing peptide. WT bone marrow cells were cultured with MCSF for 5 days, pretreated with RGD-containing peptide (20 μg/ml) for 15 min, and then treated with IGFBP1 (50 ng/ml) for 5 min. The p-ERK/t-ERK ratio was quantified as fold changes compared to lane 1 (n = 3); * compares with lane 1.

(D) Itgb1 expression was effectively diminished in osteoclast precursors from Oc-Itgb1-KO mice (n = 3).

(E and F) IGFBP1 enhancement of osteoclast differentiation was abolished in Oc-Itgb1-KO cultures.

(E) TRAP mRNA (n = 3).

(F) Images of TRAP-stained differentiation cultures. Scale bar, 25 μm. Inset shows resorptive activity by calcium release from bone into medium (mM) (n = 8); * and n.s. compare IGFBP1 with PBS control in the same genotype and culture condition.

(G) IGFBP1 induction of Erk phosphorylation was abolished in Oc-Itgb1-KO cultures (n = 3). Bone marrow cells from Oc-Itgb1-KO mice or littermate controls were cultured with MCSF for 5 days, with or without RANKL during the last 2 days and then stimulated with IGFBP1 (50 ng/ml) or vehicle control for 5 min. The

(legend continued on next page)

IGFBP1 Functions through the Integrin β1 Receptor in the Osteoclast Lineage

We next set out to identify the IGFBP1 receptor on osteoclast precursors. An arginine-glycine-aspartic acid (RGD) integrin recognition motif in the C terminus of IGFBP1 is highly conserved among mammals including human, pig, mouse, and rat (Figure 5A), indicating that IGFBP1 may function as a ligand for integrin receptors. A previous study using Chinese hamster ovary (CHO) cells reports that integrin α5β1 is the only cell surface receptor that can bind to IGFBP1 in an RGD-dependent but IGF1-independent fashion (Jones et al., 1993). We found that both IGFBP1 stimulation of osteoclastogenesis (Figure 5B) and IGFBP1 induction of Erk phosphorylation (Figure 5C) were abolished by the addition of a synthetic RGD-containing competing peptide to WT osteoclast differentiation culture. This indicates that the RGD binding motif in IGFBP1 is functionally required, suggesting that integrin α5β1 may be the IGFBP1 receptor for its pro-osteoclastogenic activity. Integrin α5 can partner with several integrin β subunits, including integrin β3, that can promote osteoclast cytoskeleton remodeling (Novack and Teitelbaum, 2008). Thus, the specificity of IGFBP1 binding likely resides in integrin β1 (Itgb1).

To determine the in vivo requirement of Itgb1 for IGFBP1 stimulation of bone resorption, we generated osteoclast-specific Itgb1 knockout mice (Oc-Itgb1-KO) by breeding Itgb1 flox mice (Raghavan et al., 2000) with lysozyme-cre transgenic mice (Clausen et al., 1999). Ex vivo bone marrow osteoclast differentiation assay showed that Itgb1 expression was reduced by 93% in the Oc-Itgb1-KO cultures, indicating efficient Itgb1 deletion (Figure 5D). Compared to control cultures, Oc-Itgb1-KO cultures were completely resistant to IGFBP1 potentiation of osteoclast differentiation but were still sensitive to RANKL-mediated and rosiglitazone-stimulated osteoclast differentiation (Figures 5E and 5F). Furthermore, IGFBP1 induction of Erk-phosphorylation was completely abolished in Oc-Itgb1-KO osteoclast precursors, whereas RANKL stimulation of Erk-phosphorylation remained intact (Figure 5G). Co-immunoprecipitation (coIP) assay showed that IGFBP1 physically interacted with Itgb1 in osteoclasts, which can be effectively blocked by anti-IGFBP1 or RGD peptide (Figure 5H). In contrast, knockdown of Itgb3 or Itgb5 did not affect the ability of IGFBP1 to potentiate osteoclast differentiation (Figure 5I). These findings reveal a functional diversity for how the β integrin family regulates osteoclastogenesis: Itgb1 promotes the early stage of osteoclast differentiation in response to IGFBP1, whereas other β integrins such as Itgb3 mainly promote the late stage of cytoskeleton remodeling (Novack and Teitelbaum, 2008).

Osteoclastic Itgb1 Deletion Abolishes IGFBP1-Induced Resorption and Bone Loss

We then analyzed the in vivo consequences by comparing Oc-Itgb1-KO mice with littermate controls, treated with IGFBP1 or vehicle control (0.015 mg/kg/day for 14 days). Consistent with the ex vivo observations, IGFBP1-induced bone resorption (Figure 6A) as well as osteoclast numbers and surface (Figure S4A) were completely abolished in Oc-Itgb1-KO mice, indicating that Itgb1 is required for the pharmacological effects of IGFBP1. Moreover, basal bone resorption (Figure 6A) as well as osteoclast numbers and surface (Figure S4A), were also significantly lower in Oc-Itgb1-KO mice compared to control mice, indicating that Itgb1 is also required for the physiological regulation by IGFBP1. In contrast, the bone formation marker P1NP (Figure 6B), osteoblast numbers/surface, bone formation rate, and mineral apposition rate (Figures S4B and S4C) were unaffected in either IGFBP1-treated mice or Oc-Itgb1-KO mice. Consequently, Oc-Itgb1-KO mice had higher basal bone mass and were refractory to IGFBP1-induced bone loss (Figures 6C, 6D, and S4D). These results indicate that Itgb1 is the major and essential β integrin receptor for IGFBP1 that accounts for its pro-osteoclastogenic function.

Deletion of the IGFBP1-Itgb1 Axis Abolishes FGF21-Induced Resorption and Bone Loss

To further investigate whether the IGFBP1-Itgb1 signaling pathway is required for FGF21-induced bone resorption and bone loss, we next examined the skeletal effects of FGF21 in Oc-Itgb1-KO mice. Oc-Itgb1-KO or control mice were fed with HFD for 5 weeks, and treated with FGF21 (1 mg/kg/day) or vehicle control during the last 14 days. In control mice, FGF21 elevated bone resorption (Figure 6E) and osteoclast number/surface (Figure S5A), leading to a lower bone mass (Figures 6F and 6G). In contrast, these effects were abolished in Oc-Itgb1-KO mice (Figures 6E–6G and S5). ITT assay revealed that FGF21-mediated insulin sensitization was intact in Oc-Itgb1-KO mice (Figure 6H). These data indicate that Itgb1 deletion in the osteoclast lineage specifically abolishes FGF21-induced bone loss detrimental effects while retaining FGF21-mediated metabolic benefits. These findings further support that Itgb1 functions as a key IGFBP1 receptor in the osteoclast lineage to mediate the resorption-enhancing effects of the FGF21-IGFBP1 axis. In accordance with our pharmacological findings, genetic rescue experiments using IGFBP1-KO/FGF21-Tg compound mutants showed that IGFBP1 deletion conferred a lower basal bone resorption and a higher basal bone mass, as well as a complete resistance to FGF21-induced bone resorption and bone loss (Figures 6I, 6K, and S6). These results further strengthen the conclusion that IGFBP1 is a physiologically significant regulator

p-ERK/t-ERK ratio was quantified as fold changes compared to lane 1 in each group of the same genotype (n = 3); black * compares with lane 1 in each group; blue * or n.s. compares with "no IGFBP1, RANKL only" in lane 3 in each group.

(H) CoIP analysis of IGFBP1 binding to Itgb1 in osteoclasts and its blockade by anti-IGFBP1 and RGD peptide. CoIP was performed with anti-Itgb1 or IgG control; IGFBP1 was released from the complex and then quantified by ELISA (n = 3). Black * and n.s. compare with column 1; blue + compares with column 2.

(I) Knockdown of Itgb3 or Itgb5 does not affect IGFBP1 induction of osteoclast differentiation. Bone marrow osteoclast differentiation cultures were transfected with siRNA before RANKL induction, and expression of Itgb3 (top left), Itgb5 (top right), and TRAP differentiation marker (bottom) was quantified by RT-QPCR (n = 6). TRAP mRNA in Oc-Itgb1-KO cells serves as a positive control.

Statistical analyses were performed with Student's t test and are shown as mean ± SD. *$p < 0.05$; **$p < 0.01$; ***$p < 0.005$; ****$p < 0.001$; n.s., non-significant ($p > 0.05$).

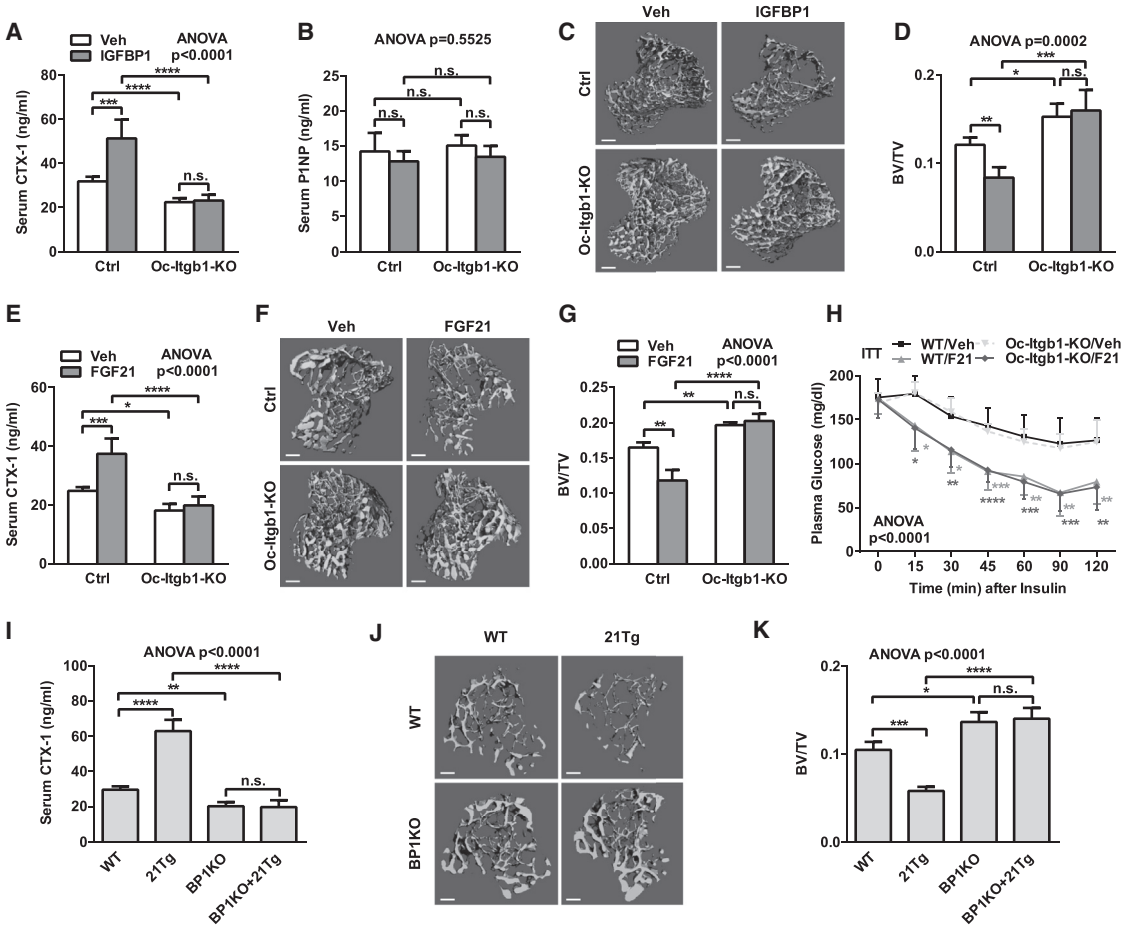

Figure 6. Osteoclastic Itgb1 Deletion Abolishes IGFBP1- and FGF21-induced Bone Resorption and Bone Loss

(A–D) IGFBP1 induction of bone resorption and bone loss was abolished in Oc-Itgb1-KO mice. Oc-Itgb1-KO mice or littermate controls (2-month-old, male, n = 6) were treated with IGFBP1 (0.015 mg/kg/day) or PBS for 14 days.

(A) Serum CTX-1.

(B) Serum P1NP.

(C) μCT images of the trabecular bone of the tibial metaphysis. Scale bar, 10 μm.

(D) Trabecular BV/TV.

(E–H) Osteoclastic Itgb1 deletion abolishes FGF21-induced bone loss while retaining FGF21-induced insulin sensitization. Oc-Itgb1-KO mice or littermate controls (3-month-old, male, n = 6) were fed with HFD for 5 weeks, and treated with FGF21 (1 mg/kg/day) during the last 14 days.

(E) Serum CTX-1.

(F) μCT images of the trabecular bone of the tibial metaphysis. Scale bar, 10 μm.

(G) Trabecular BV/TV.

(H) ITT assay. Mice were fasted for 4 hr and then received a single IP injection of FGF21 (1 mg/kg) or vehicle control, co-injected with insulin (0.75 U/kg).

(I–K) Comparison of WT, FGF21-Tg, IGFBP1-KO, and IGFBP1-KO/FGF21-Tg mice (2-month-old, male, n = 6).

(I) Serum CTX-1.

(J) μCT images of the trabecular bone of the tibial metaphysis. Scale bar, 10 μm.

(K) Trabecular BV/TV.

Statistical analyses were performed with Student's t test or ANOVA followed by the post hoc Tukey pairwise comparisons; error bars indicate SD. *$p < 0.05$; **$p < 0.01$; ***$p < 0.005$; ****$p < 0.001$; n.s., non-significant ($p > 0.05$). See also Figures S4–S6.

of bone resorption, and the key Itgb1 ligand that mediates FGF21-induced bone resorption.

DISCUSSION

This study uncovers a crucial liver-bone endocrine relay, as well as a key mechanism for FGF21-induced bone resorption. Physiological or pharmacological elevation of FGF21 induces IGFBP1 expression in the liver and its secretion into circulation. In turn, IGFBP1 acts directly on the osteoclast precursors by binding to integrin β1 receptor via its RGD motif. Consequently, IGFBP1 stimulates osteoclast differentiation and bone resorption by potentiating RANKL-induced Erk phosphorylation and NFATc1 activation, leading to lower bone mass (Figure 7). Thus, we have identified IGFBP1 as an endocrine hormone that is secreted from the liver in response

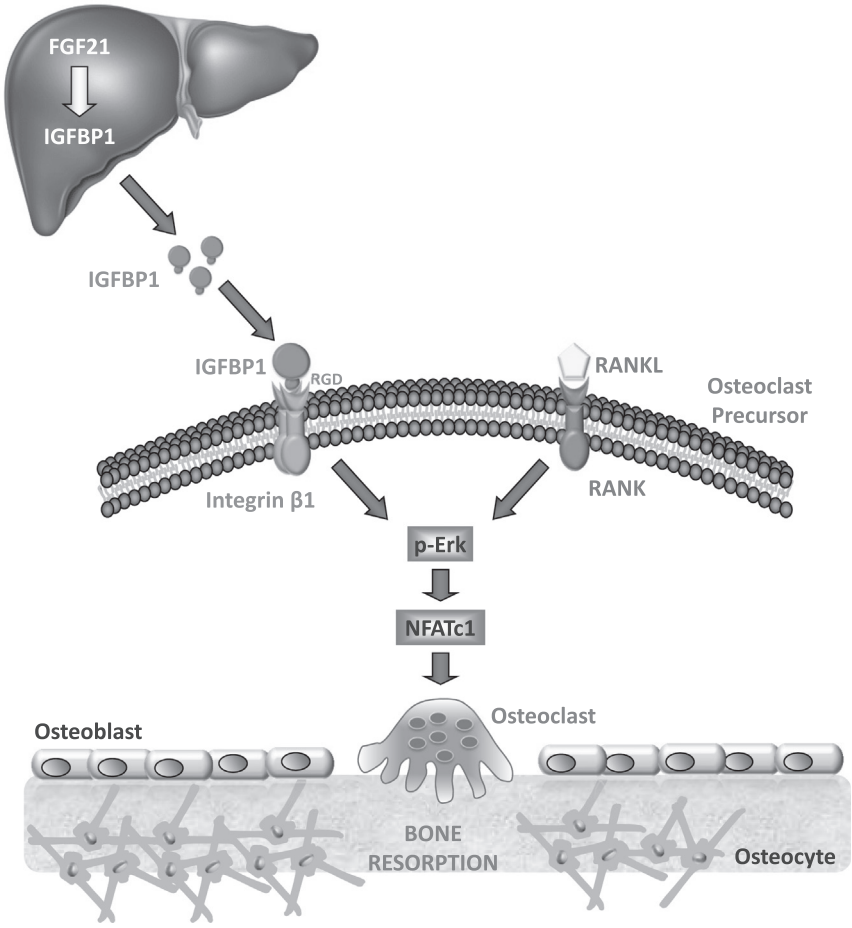

Figure 7. A Simplified Model for How the Liver Hormone IGFBP1 Regulates Osteoclast Differentiation and Mediates FGF21-Induced Bone Resorption

FGF21 induces liver expression and secretion of IGFBP1. IGFBP1 in turn functions as an endocrine hormone by binding to its receptor integrin β1 on the osteoclast precursors, leading to the potentiation of RANKL signaling and enhanced osteoclast differentiation. Consequently, a physiological or pharmacological elevation of FGF21 levels results in a higher circulating IGFBP1 level, leading to increased bone resorption and bone loss.

to metabolic cues to regulate bone resorption and skeletal homeostasis.

Our findings reveal that an anti-IGFBP1 antibody can suppress bone resorption and increase bone mass, highlighting pharmacological IGFBP1 blockade as a potential strategy for the treatment of osteoporosis. Moreover, we have also identified the IGFBP1-Itgb1 pathway as an essential and specific mediator of FGF21-induced bone resorption; either an IGFBP1-blocking antibody or osteoclastic Itgb1 deletion confers resistance to FGF21-induced bone loss without compromising its insulin-sensitizing benefits. These findings suggest that pharmacological IGFBP1 blockade may also represent a potential avenue to ameliorate the detrimental skeletal effects of FGF21 while preserving its beneficial metabolic actions. Our previous study shows that FGF21 inhibits osteoblast differentiation via a direct effect on the mesenchymal lineage by favoring marrow adipogenesis (Wan, 2013; Wei et al., 2012). Here we show that FGF21 stimulates osteoclast differentiation via an indirect liver-bone hormonal relay by IGFBP1. Therefore, two distinct mechanisms mediate the two different aspects of FGF21 regulation of bone remodeling.

Our data show that IGFBP1 alone can stimulate Erk phosphorylation and further enhance RANKL-induced Erk phosphorylation (Figures 4D, 4E, and 5G) without affecting c-Jun phosphorylation, Akt phosphorylation, or IκBα degradation (Figure 4F). The reason that IGFBP1 only stimulates osteoclastogenesis in the presence of RANKL is that although pErk can promote osteoclast differentiation, it is not sufficient to trigger the entire program of differentiation, which also requires the other RANKL downstream signaling pathways. Thus, in the absence of RANKL, IGFBP1 can stimulate pErk but not osteoclast differentiation, but in the presence of RANKL, IGFBP1-potentiated pErk can enhance RANKL-mediated osteoclast differentiation.

Our findings reveal that IGFBP1 functions as a pro-osteoclastogenic liver hormone via the Itgb1 receptor in osteoclasts but independent of IGF1, as well as a key mediator of FGF21-induced bone resorption and bone loss. A previous study shows that IGFBP2 can also enhance osteoclast differentiation (DeMambro et al., 2012). Although IGFBP2 is highly expressed in osteoblasts, it is also expressed in liver, suggesting that its resorption-enhancing activity may partially stem from the liver, which has never been previously recognized and still awaits future investigation. Moreover, IGFBP2 also contains a similar RGD region, suggesting that its pro-osteoclastogenic function may be also mediated by integrin receptors. The robust induction of liver IGFBP1 expression by FGF21 has been well described (Inagaki et al., 2008), although FGF21 induction of IGFBP2 has also been reported (Emanuelli et al., 2014). We found that liver IGFBP2 mRNA were not significantly altered by 3 days of FGF21 treatment versus vehicle control (1.2-fold, $p = 0.25$) and neither was serum IGFBP2 levels (1.06-fold, $p = 0.49$). Importantly, the complete abolishment of FGF21-induced bone resorption both in IGFBP1-KO mice and anti-IGFBP1-treated mice demonstrates that IGFBP1 is the major mediator of FGF21 enhancement of osteoclastogenesis, whereas IGFBP2 plays only a minor role, if any. Although basal bone formation is unaffected by IGFBP1 blockade or osteoclastic Itgb1 deletion, FGF21 inhibition of bone formation is dampened (Figures S3B, S3C, S5B, S5C, S6B, and S6C), which in combination with the impairment of FGF21 augmentation of bone resorption alleviates the uncoupling effects and FGF21-induced bone loss.

The increase in circulating IGFBP1 levels upon OVX and the abolishment of OVX-induced bone resorption by IGFBP1

blockade suggest that estrogen may protect bone by suppressing IGFBP1-mediated pathological bone resorption. Although the major physiological effect of estrogen is to inhibit bone resorption, bone formation also changes following estrogen deficiency. In our experiments in mice, we observed a reduction in bone formation 5 weeks after OVX compared with sham controls (Figure 3C). A previous study in rat reported that bone formation was decreased during the first week post-OVX and then increased during third and fourth weeks post-OVX (Tanizawa et al., 2000). We do not know why this discrepancy occurs.

An early study failed to detect any osteoclast differentiation defects in Itgb1-deficient cells (Schmidt et al., 2011). Potential explanations for this discrepancy are (1) the Itgb1-deficient mice in this early study were generated with MX1-cre after a single dose of pI/pC injection, and it was unclear how efficient Itgb1 was deleted; (2) the heat-inactivated FCS they used in the differentiation cultures might have much less active IGFBP1 than the FBS we used; and (3) their study was entirely in vitro without any in vivo examination of bone resorption, osteoclast number, or bone mass. A recent study showed that deletion of DAP12 had no effect on bone mass relative to WT nor did additional deletion of Itgb1 in osteoclast lineage cells on a *DAP12*$^{-/-}$ background (Zou and Teitelbaum, 2015). The source of this discrepancy is unclear.

Integrin receptors are important effectors of not only cell adhesion and migration but also cell differentiation. Particularly, integrin β1 has been reported to regulate neuronal and astrocytic differentiation (Pan et al., 2014; Tate et al., 2004), keratinocyte differentiation (Hotchin et al., 1995; Levy et al., 2000), type II lung epithelial cell differentiation (Sanchez-Esteban et al., 2006), chondrogenesis (Singh and Schwarzbauer, 2012), and mammary epithelium differentiation (Naylor et al., 2005). Here we uncover IGFBP1 as a functional circulating ligand for integrin β1, in addition to the previously reported extracellular matrix ligands such as fibronectin. Importantly, our current genetic and biochemical studies have established integrin β1 as a critical IGFBP1 receptor that is essential for its pro-osteoclastogenic function.

Several human diseases including osteoporosis and diabetes are associated with higher serum IGFBP1 levels and at the same time bone loss (Jehle et al., 2003; Miao et al., 2005; Moyer-Mileur et al., 2008; Rosen, 2008; Ruan and Lai, 2010; Salminen et al., 2008; Schwartz et al., 2001), although a lack of correlation has also been reported (Pye et al., 2011). Nonetheless, the functional significance and molecular mechanisms underlying IGFBP1 actions in these clinical observations have been long elusive. This study challenges the dogma that IGFBP1 regulates physiology solely as an IGF1 binder by revealing its function as an endocrine hormone. A quarter of century after its cloning, IGFBP1 is now recognized as a metabolic signal sent from the liver to the bone to directly stimulate osteoclastogenesis and bone resorption via the receptor integrin β1. This discovery paves the road for future investigations of how IGFBP1 is regulated under various physiological and pathological conditions. In addition to FGF21, IGFBP1 levels may be also modulated by other upstream signals—the observation that OVX induces IGFBP1 indicates that estrogen may directly or indirectly suppress liver IGFBP1 expression. Moreover, this discovery provides key insights for how skeletal homeostasis may be modulated via changes in IGFBP1. For example, IGFBP1 levels is suppressed by insulin and increased in type 1 diabetes (Lee et al., 1993); it is also stimulated by glucocorticoids (Goswami et al., 1994). Intriguingly, our findings indicate that IGFBP1 blockade may specifically prevent the excessive bone resorption without completely eliminating RANKL-mediated physiological basal bone resorption, which is essential for bone regeneration and fracture repair. Hence, the discovery of IGFBP1 as an FGF21-induced pro-osteoclastogenic liver hormone opens an exciting new path to the fundamental understanding of the physiological and pathological connection between energy metabolism and skeletal homeostasis, as well as the development of new pharmacological treatments of bone and metabolic diseases.

EXPERIMENTAL PROCEDURES

Mice

FGF21-Tg mice (Ding et al., 2012; Inagaki et al., 2007) and IGFBP1-KO mice (Leu et al., 2003) on a C57BL6 background have been described. Osteoclastic integrin β1 KO mice were generated by crossing Integrin β1 flox mice (Raghavan et al., 2000) with lysozyme-cre mice (Clausen et al., 1999) (Jackson laboratory). OVX or sham operation was performed as described (Wei et al., 2011). ITT was performed as described (Ding et al., 2012). Mice were fed standard chow containing 4% fat ad libitum unless stated otherwise. For diet-induced-obesity, mice were fed a HFD containing 60% kcal from fat (Research Diets Inc. #D12492). All experiments were conducted using littermates. Sample size estimate was based on power analyses performed using SAS 9.3 TS X64_7PRO platform at the UTSW Biostatistics Core. With the observed group differences and the relatively small variation of the in vivo measurements, a sample size of four per group (n = 4) and three per group (n = 3) will provide >90% and >80% power at type I error rate of 0.05 (two-sided test), respectively. All animal experiments were approved by the Institutional Animal Care and Use Committee of the University of Texas Southwestern Medical Center.

Reagent

Recombinant mouse IGFBP1 (1588-B1-025), human IGFBP1 (871-B1-025), mouse RANKL (462-TR), human RANKL (390-TN-010), mouse MCSF (416-ML), as well as anti-IGFBP1 antibody (AF1240) were from R&D Systems. RGD-containing peptide (Gly-Arg-Gly-Asp-Thr-Pro) was from Sigma. Antibodies for p-ERK (#9101), total ERK (#4695), p-Akt (#4058), total-Akt (#2920), p-c-Jun (#9164), and total c-Jun (#9165) were from Cell Signaling; antibodies for IκBα (sc-371) and Itgb1 (sc-8978) were from Santa Cruz Biotechnology. RAW264.7 mouse macrophage cell line was from ATCC (TIB-71). Serum and cellular IGFBP1 was quantified by ELISA (Abnova, KA3054). Total and free serum IGF1 was quantified by ELISA (ALPCO, 22-IG1MS-E01).

Bone Analyses

μCT was performed to evaluate bone volume and architecture using a Scanco μCT-35 instrument (SCANCO Medical) as described (Wei et al., 2010, 2012). Bone histomorphometry was performed as described (Wei et al., 2012). As a bone resorption marker, serum CTX-1 was measured with the RatLaps™ EIA kit (Immunodiagnostic Systems) (Wei et al., 2012). As a bone formation marker, serum PINP was measured with the Rat/Mouse PINP EIA kit (Immunodiagnostic Systems) (Wei et al., 2012).

Bone Marrow Osteoclast Differentiation

Osteoclasts were differentiated from mouse bone marrow cells as described (Wan et al., 2007; Wei et al., 2010). Briefly, hematopoietic bone marrow cells were purified with 40 μm cell strainer and differentiated with 40 ng/ml of mouse M-CSF (R&D Systems) in α-MEM containing 10% FBS for 3 days, then with 40 ng/ml of mouse MCSF and 100 ng/ml of mouse RANKL (R&D Systems) for 3–9 days, with or without rosiglitazone (1 μM). The FBS contained bovine IGFBPs including IGFBP1 and IGFBP3-bound IGF1. Mature osteoclasts were identified as multinucleated (>3 nuclei) TRAP^{+} cells. Osteoclast differentiation was quantified by the RNA expression of osteoclast marker genes

using RT-QPCR, normalized by the L19 ribosomal protein gene. For osteoclast resorptive function analyses, osteoclast differentiation was conducted in OsteoAssay bone plates (Lonza) (n = 8 wells per condition), and osteoclast activity was quantified as calcium release from bone into culture medium using CalciFluo ELISA assay (Lonza); "−RANKL" and "+RANKL" served as negative and positive controls, respectively. Each experiment was repeated for three times, and representative results are shown. Osteoblast differentiation was conducted as described (Wei et al., 2012). For all bone cell differentiation, similar results were observed using bone marrow cells from male or female mice, and representative results from male mice are shown. To determine the effects of liver-secreted factors on osteoclast differentiation, fresh liver was minced in culture medium (α-MEM+10% FBS) and dispersed by gentle vortex for 5 min; cells were pelleted by centrifugation at 10,000 rpm for 10 min; supernatant was collected as LCM and used to treat osteoclast differentiation culture. Human PBMN cells (ReachBio) were differentiated into osteoclasts in α-MEM containing 10% FBS, 25 ng/ml MCSF, 50 ng/ml hRANKL, 1 μM dexamethasome, and 1 μM rosiglitazone for 14 days, in the presence of 5 ng/ml human IGFBP1 or PBS control.

Statistical Analyses

All statistical analyses were performed with Student's t test and presented as mean ± SD unless stated otherwise. For in vivo experiments with ≥3 groups, statistical analyses were performed with ANOVA followed by the post hoc Tukey pairwise comparisons. The p values were designated as * $p < 0.05$, ** $p < 0.01$, *** $p < 0.005$, and **** $p < 0.001$; n.s., non-significant ($p > 0.05$).

SUPPLEMENTAL INFORMATION

Supplemental Information includes six figures and can be found with this article online at http://dx.doi.org/10.1016/j.cmet.2015.09.010.

AUTHOR CONTRIBUTIONS

X.W., W.W., and Y. Wan conceived the project and designed the experiments. X.W. and W.W. conducted most of the experiments and data analyses. J.Y.K. assisted with OVX. Y. Wang assisted with coIP. Y. Wan wrote the manuscript.

ACKNOWLEDGMENTS

We thank Drs. David Mangelsdorf and Steve Kliewer (UT Southwestern) for FGF21-Tg mice and Drs. Paul Dechow and Jerry Feng (Baylor College of Dentistry at Dallas) for assistance with μCT and histomorphometry analyses. Y. Wan is a Virginia Murchison Linthicum Scholar in Medical Research. This work was in part supported by NIH (R01DK089113, Y. Wan), The Welch Foundation (I-1751, Y. Wan), and the UT Southwestern Endowed Scholar Startup Fund (Y. Wan). The authors declare that they have no financial conflict of interest.

Received: January 23, 2015
Revised: May 26, 2015
Accepted: September 9, 2015
Published: October 8, 2015

REFERENCES

Cantó, C., and Auwerx, J. (2012). Cell biology. FGF21 takes a fat bite. Science *336*, 675–676.

Choi, S.W., Park, K.I., Yeon, J.T., Ryu, B.J., Kim, K.J., and Kim, S.H. (2014). Anti-osteoclastogenic activity of matairesinol via suppression of p38/ERK-NFATc1 signaling axis. BMC Complement. Altern. Med. *14*, 35.

Clausen, B.E., Burkhardt, C., Reith, W., Renkawitz, R., and Förster, I. (1999). Conditional gene targeting in macrophages and granulocytes using LysMcre mice. Transgenic Res. *8*, 265–277.

DeMambro, V.E., Maile, L., Wai, C., Kawai, M., Cascella, T., Rosen, C.J., and Clemmons, D. (2012). Insulin-like growth factor-binding protein-2 is required for osteoclast differentiation. J. Bone Miner. Res. *27*, 390–400.

Ding, X., Boney-Montoya, J., Owen, B.M., Bookout, A.L., Coate, K.C., Mangelsdorf, D.J., and Kliewer, S.A. (2012). βKlotho is required for fibroblast growth factor 21 effects on growth and metabolism. Cell Metab. *16*, 387–393.

Emanuelli, B., Vienberg, S.G., Smyth, G., Cheng, C., Stanford, K.I., Arumugam, M., Michael, M.D., Adams, A.C., Kharitonenkov, A., and Kahn, C.R. (2014). Interplay between FGF21 and insulin action in the liver regulates metabolism. J. Clin. Invest. *124*, 515–527.

Goswami, R., Lacson, R., Yang, E., Sam, R., and Unterman, T. (1994). Functional analysis of glucocorticoid and insulin response sequences in the rat insulin-like growth factor-binding protein-1 promoter. Endocrinology *134*, 736–743.

Hotchin, N.A., Gandarillas, A., and Watt, F.M. (1995). Regulation of cell surface beta 1 integrin levels during keratinocyte terminal differentiation. J. Cell Biol. *128*, 1209–1219.

Inagaki, T., Dutchak, P., Zhao, G., Ding, X., Gautron, L., Parameswara, V., Li, Y., Goetz, R., Mohammadi, M., Esser, V., et al. (2007). Endocrine regulation of the fasting response by PPARalpha-mediated induction of fibroblast growth factor 21. Cell Metab. *5*, 415–425.

Inagaki, T., Lin, V.Y., Goetz, R., Mohammadi, M., Mangelsdorf, D.J., and Kliewer, S.A. (2008). Inhibition of growth hormone signaling by the fasting-induced hormone FGF21. Cell Metab. *8*, 77–83.

Jehle, P.M., Schulten, K., Schulz, W., Jehle, D.R., Stracke, S., Manfras, B., Boehm, B.O., Baylink, D.J., and Mohan, S. (2003). Serum levels of insulin-like growth factor (IGF)-I and IGF binding protein (IGFBP)-1 to -6 and their relationship to bone metabolism in osteoporosis patients. Eur. J. Intern. Med. *14*, 32–38.

Jones, J.I., Gockerman, A., Busby, W.H., Jr., Wright, G., and Clemmons, D.R. (1993). Insulin-like growth factor binding protein 1 stimulates cell migration and binds to the alpha 5 beta 1 integrin by means of its Arg-Gly-Asp sequence. Proc. Natl. Acad. Sci. USA *90*, 10553–10557.

Key, T.J., Appleby, P.N., Reeves, G.K., and Roddam, A.W.; Endogenous Hormones and Breast Cancer Collaborative Group (2010). Insulin-like growth factor 1 (IGF1), IGF binding protein 3 (IGFBP3), and breast cancer risk: pooled individual data analysis of 17 prospective studies. Lancet Oncol. *11*, 530–542.

Kim, H.J., Lee, Y., Chang, E.J., Kim, H.M., Hong, S.P., Lee, Z.H., Ryu, J., and Kim, H.H. (2007). Suppression of osteoclastogenesis by N,N-dimethyl-D-erythro-sphingosine: a sphingosine kinase inhibition-independent action. Mol. Pharmacol. *72*, 418–428.

Krum, S.A. (2011). Direct transcriptional targets of sex steroid hormones in bone. J. Cell. Biochem. *112*, 401–408.

Lee, P.D., Conover, C.A., and Powell, D.R. (1993). Regulation and function of insulin-like growth factor-binding protein-1. Proc. Soc. Exp. Biol. Med. *204*, 4–29.

Leu, J.I., Crissey, M.A., Craig, L.E., and Taub, R. (2003). Impaired hepatocyte DNA synthetic response posthepatectomy in insulin-like growth factor binding protein 1-deficient mice with defects in C/EBP beta and mitogen-activated protein kinase/extracellular signal-regulated kinase regulation. Mol. Cell. Biol. *23*, 1251–1259.

Levy, L., Broad, S., Diekmann, D., Evans, R.D., and Watt, F.M. (2000). beta1 integrins regulate keratinocyte adhesion and differentiation by distinct mechanisms. Mol. Biol. Cell *11*, 453–466.

Miao, J., Brismar, K., Nyrén, O., Ugarph-Morawski, A., and Ye, W. (2005). Elevated hip fracture risk in type 1 diabetic patients: a population-based cohort study in Sweden. Diabetes Care *28*, 2850–2855.

Moyer-Mileur, L.J., Slater, H., Jordan, K.C., and Murray, M.A. (2008). IGF-1 and IGF-binding proteins and bone mass, geometry, and strength: relation to metabolic control in adolescent girls with type 1 diabetes. J. Bone Miner. Res. *23*, 1884–1891.

Nakamura, T., Imai, Y., Matsumoto, T., Sato, S., Takeuchi, K., Igarashi, K., Harada, Y., Azuma, Y., Krust, A., Yamamoto, Y., et al. (2007). Estrogen prevents bone loss via estrogen receptor alpha and induction of Fas ligand in osteoclasts. Cell *130*, 811–823.

Naylor, M.J., Li, N., Cheung, J., Lowe, E.T., Lambert, E., Marlow, R., Wang, P., Schatzmann, F., Wintermantel, T., Schüetz, G., et al. (2005). Ablation of beta1

integrin in mammary epithelium reveals a key role for integrin in glandular morphogenesis and differentiation. J. Cell Biol. *171*, 717–728.

Novack, D.V., and Teitelbaum, S.L. (2008). The osteoclast: friend or foe? Annu. Rev. Pathol. *3*, 457–484.

Pan, L., North, H.A., Sahni, V., Jeong, S.J., Mcguire, T.L., Berns, E.J., Stupp, S.I., and Kessler, J.A. (2014). β1-Integrin and integrin linked kinase regulate astrocytic differentiation of neural stem cells. PLoS ONE *9*, e104335.

Potthoff, M.J., Kliewer, S.A., and Mangelsdorf, D.J. (2012). Endocrine fibroblast growth factors 15/19 and 21: from feast to famine. Genes Dev. *26*, 312–324.

Pye, S.R., Almusalam, B., Boonen, S., Vanderschueren, D., Borghs, H., Gielen, E., Adams, J.E., Ward, K.A., Bartfai, G., Casanueva, F.F., et al.; EMAS Study Group (2011). Influence of insulin-like growth factor binding protein (IGFBP)-1 and IGFBP-3 on bone health: results from the European Male Ageing Study. Calcif. Tissue Int. *88*, 503–510.

Raghavan, S., Bauer, C., Mundschau, G., Li, Q., and Fuchs, E. (2000). Conditional ablation of beta1 integrin in skin. Severe defects in epidermal proliferation, basement membrane formation, and hair follicle invagination. J. Cell Biol. *150*, 1149–1160.

Rosen, C.J. (2008). Sugar and bone: a not-so sweet story. J. Bone Miner. Res. *23*, 1881–1883.

Ruan, W., and Lai, M. (2010). Insulin-like growth factor binding protein: a possible marker for the metabolic syndrome? Acta Diabetol. *47*, 5–14.

Salminen, H., Saaf, M., Ringertz, H., and Strender, L.E. (2008). The role of IGF-I and IGFBP-1 status and secondary hyperparathyroidism in relation to osteoporosis in elderly Swedish women. Osteoporos. Int. *19*, 201–209.

Sanchez-Esteban, J., Wang, Y., Filardo, E.J., Rubin, L.P., and Ingber, D.E. (2006). Integrins beta1, alpha6, and alpha3 contribute to mechanical strain-induced differentiation of fetal lung type II epithelial cells via distinct mechanisms. Am. J. Physiol. Lung Cell. Mol. Physiol. *290*, L343–L350.

Schmidt, S., Nakchbandi, I., Ruppert, R., Kawelke, N., Hess, M.W., Pfaller, K., Jurdic, P., Fässler, R., and Moser, M. (2011). Kindlin-3-mediated signaling from multiple integrin classes is required for osteoclast-mediated bone resorption. J. Cell Biol. *192*, 883–897.

Schwartz, A.V., Sellmeyer, D.E., Ensrud, K.E., Cauley, J.A., Tabor, H.K., Schreiner, P.J., Jamal, S.A., Black, D.M., and Cummings, S.R.; Study of Osteoporotic Features Research Group (2001). Older women with diabetes have an increased risk of fracture: a prospective study. J. Clin. Endocrinol. Metab. *86*, 32–38.

Singh, P., and Schwarzbauer, J.E. (2012). Fibronectin and stem cell differentiation - lessons from chondrogenesis. J. Cell Sci. *125*, 3703–3712.

Stolzenberg-Solomon, R.Z., Limburg, P., Pollak, M., Taylor, P.R., Virtamo, J., and Albanes, D. (2004). Insulin-like growth factor (IGF)-1, IGF-binding protein-3, and pancreatic cancer in male smokers. Cancer Epidemiol. Biomarkers Prev. *13*, 438–444.

Tanizawa, T., Yamaguchi, A., Uchiyama, Y., Miyaura, C., Ikeda, T., Ejiri, S., Nagal, Y., Yamato, H., Murayama, H., Sato, M., and Nakamura, T. (2000). Reduction in bone formation and elevated bone resorption in ovariectomized rats with special reference to acute inflammation. Bone *26*, 43–53.

Tate, M.C., García, A.J., Keselowsky, B.G., Schumm, M.A., Archer, D.R., and LaPlaca, M.C. (2004). Specific beta1 integrins mediate adhesion, migration, and differentiation of neural progenitors derived from the embryonic striatum. Mol. Cell. Neurosci. *27*, 22–31.

Wan, Y. (2013). Bone marrow mesenchymal stem cells: fat on and blast off by FGF21. Int. J. Biochem. Cell Biol. *45*, 546–549.

Wan, Y., Chong, L.W., and Evans, R.M. (2007). PPAR-gamma regulates osteoclastogenesis in mice. Nat. Med. *13*, 1496–1503.

Wei, W., Wang, X., Yang, M., Smith, L.C., Dechow, P.C., Sonoda, J., Evans, R.M., and Wan, Y. (2010). PGC1beta mediates PPARgamma activation of osteoclastogenesis and rosiglitazone-induced bone loss. Cell Metab. *11*, 503–516.

Wei, W., Zeve, D., Wang, X., Du, Y., Tang, W., Dechow, P.C., Graff, J.M., and Wan, Y. (2011). Osteoclast progenitors reside in the peroxisome proliferator-activated receptor γ-expressing bone marrow cell population. Mol. Cell. Biol. *31*, 4692–4705.

Wei, W., Dutchak, P.A., Wang, X., Ding, X., Wang, X., Bookout, A.L., Goetz, R., Mohammadi, M., Gerard, R.D., Dechow, P.C., et al. (2012). Fibroblast growth factor 21 promotes bone loss by potentiating the effects of peroxisome proliferator-activated receptor γ. Proc. Natl. Acad. Sci. USA *109*, 3143–3148.

Zou, W., and Teitelbaum, S.L. (2015). Absence of Dap12 and the αvβ3 integrin causes severe osteopetrosis. J. Cell Biol. *208*, 125–136.